Relationship between powder properties and powder layer quality in powder-bed-based additive manufacturing processes.

M.Soulier mathieu.soulier@cea.fr, A. Burr, M.Roumanie, V. Bonnefoy, R. Laucournet
Univ. Grenoble Alpes, CEA, Liten, F-38000 Grenoble, France.

Abstract
The powder spreadability drives the robustness of powder-bed-based additive manufacturing processes (laser powder bed fusion and binder jetting) as well as the performance of the printed parts. A data analysis relying on the characterizations of 59 powders is introduced to better understand and predict powder spreadability. The study is also supported by data coming from a powder spreading bench able to assess the powder layer roughness and apparent density.
It is found that the untapped powder apparent density is a relevant indicator of the powder layer density. The untapped density is itself widely dependent on the particle sphericity measured by morphogranulometry. A statistical model based on multiple linear regressions and standard least square method has been established to predict powder apparent density based on the particle shape and size. The model explains 85% of the variability of the relative powder apparent density and allows an efficient screening of powders spreadability without experiments.
A comparison between roller-spreading and blade-spreading is also presented in the study. The compacting forces applied by the roller on the powder bed allow the spreading of fine cohesive powder below 15 microns, which is impossible with a blade. Spreading of such fine powder presents the advantage to minimize the powder layer roughness.

Introduction

Laser Powder Bed Fusion (L-PBF)[1] and Binder Jetting (BJ)[2] are two powder bed based additive manufacturing (PBB-AM) processes which enable the manufacturing of complex shaped metallic parts. PBB-AM techniques rely on iterative spreading of thin powders layers intended to be either selective melted by a laser (L-PBF) or by particles adhesions by droplets of binder ejected by a printer head.
Both technologies requires a fine control of powder characteristics to master a reproducible spreadability of powder layers and ensure the robustness of the process. Moreover particle size and shape are the main drivers of the powder packing density, influencing the interparticle friction[3]. Many studies point out the impact of the particles on powder bed densities[4-7] and powder bed flowability[8,9]. In L-PBF process, a poor powder packing makes increase the required lasing energy to elaborate full dense parts[10] and may lead to residual porosities[11] or higher part roughness[12]. In BJ process, the powder bed apparent density is driving the mechanical strength of the printed green part and the final part density[2].

Most of these studies assessed on a case-by-case basis the effect of powder properties on powder processability for PBB-AM processes through several typical powder characterizations (particle size distribution so-called PSD, particle shape, apparent density, flowability). Relying on a database including more than 50 stainless steel powders with various PSD and particle shape, the first aim of this study is first to propose a statistical model relating the particle size and shape and as a response of the model the powder apparent density. The second aim is to present a powder spreading investigation performed thanks to an innovative powder spreading bench allowing to evaluate powder layer roughness and apparent density.

1) Database of stainless steel powders

The powder database includes 59 stainless-steel powders (316L). These commercial gas or water-atomized powders are covering a large range of particle sizes and shapes encountered in powder metallurgy processes. Most of them are dedicated to L-PBF and BJ but some of them are used in metal injection molding or conventional sintering.

For each powder of the database, the particle size distribution is evaluated by laser granulometry in ethanol (*Malvern Mastersizer 2000*). The particle morphology is assessed by automated image analysis on 50 000 particles (morphogranulometer, *Malvern Morpho G3*). The corresponding shape indicator studied is the mean aspect ratio defined as the width to length particle ratio. The panel of the powder database is depicted

Figure 1.

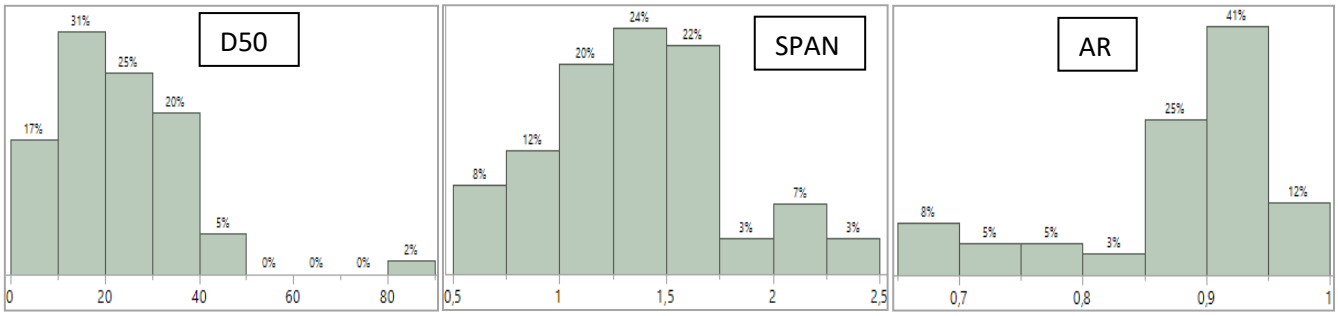

Figure 1: Stainless steel database including 59 powders: D50 (average particle size), SPAN ((D90-D10)/D50) and AR (particle median aspect ratio).

The first analysis proposed is to evaluate the relationship between above-mentioned powder characteristics and powder flowability (avalanche angle) or powder packing (tap/untapped density). The avalanche angle measurements were performed in a drum rotating at 0.6 rpm (*Mercury Scientific, Revolution*). Apparent density is measured using a scott volumeter (*Landgraf HLL, ISO 3923-2*). Tapped density is assessed using the ISO3953 standard (*Quantachrome Autotap*).

a) b)

T*ure 2* displays a matrix assessing the linear c tion between two variables.

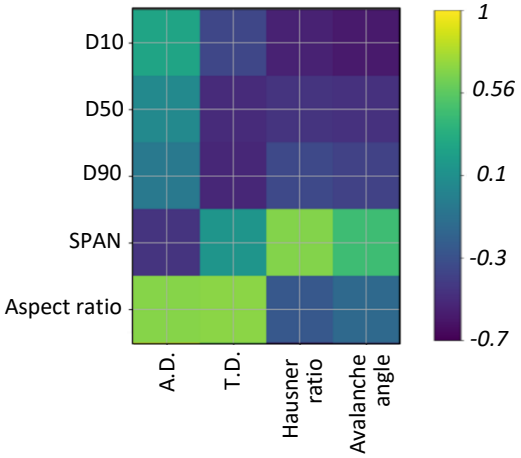

	Untaped density	Tapped density	Hausner ratio	Avalanche angle
D10	0.29	-0.35	-0.56	-0.60
D50	*	-0.51	-0.46	-0.48
D90	*	-0.52	-0.34	-0.38
SPAN	-0.46	*	0.68	0.46
Aspect ratio	0.68	0.70	*	*

*Figure 2: a): Linear correlation matrix between PSD (D10, D50, D90, SPAN), Aspect ratio and apparent density (A.D.), tapped density (T.D.), Hausner ratio (tapped/untapped density) and avalanche angle measurements. b): Table of corresponding Pearson coefficient for each linear correlation. Correlations denoted by * are not significantly different from 0.*

The powder packing (A.D. and T.D.) is firstly correlated and increasing with the particle sphericity (R_{xy} ~ +0.7). This result is in agreement with the theory of particle packing [3]. However, within the panel of powders studied, the particle shape has a marginal contribution on powder flowability (Hausner ratio and avalanche angle). Indeed, the parameter that really drives the flowability is the particle size distribution. Quite logically, the powder flowability is improved as the deciles D10, D50 and D90 are increasing. We can notice that the fine content in the PSD (D10) has a higher impact than the D50 and D90.

The

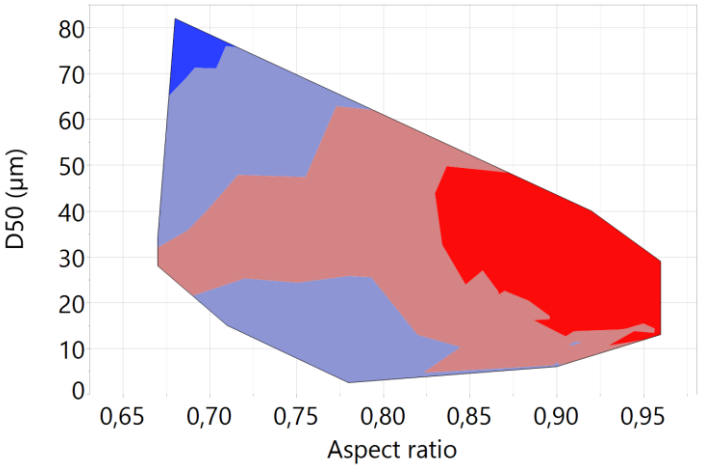

Figure 3 gives an overview of the untapped apparent measurements for the 59 powders of the database, according to their average particle size and particle shape. The white domains in the graph are not explored by the powder database. This macro-representation points out clearly the positive effect of particle sphericity on the untapped density. Indeed, powder apparent density higher than 50% are reached for particle aspect ratio larger than 0.85. Apparent density larger than 50% (red domain in the map below) is recommended in particular for BJ process [2]. Within this domain, when the particle size decreases, the particle aspect ratio becomes larger to remain above 50% density. Indeed, a higher particle sphericity is required to overcome the increase of the interparticle friction caused by the lower granulometry.

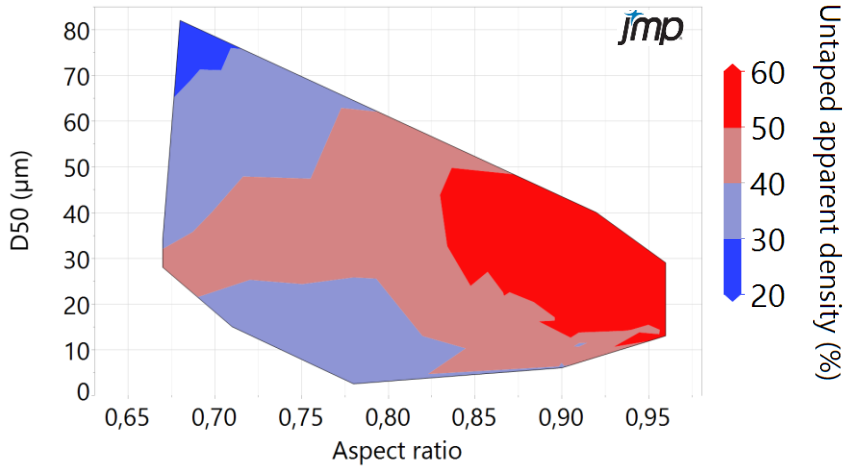

Figure 3: Contour plot graphic showing the untapped powder apparent density according to the average particle size (D50) and particle mean aspect ratio.

To go further, a statistical model has been established to predict a powder apparent density based on its properties. To this end, a multiple linear regression was performed based on standard least square method. The fit model is linking powder apparent density on one-hand and powder characteristics having significant effect on the model response on the other hand (including interaction terms and term of degree two if they are significant).

As a result, the model explains 85% of the variability of the response (R^2). The established equation allows to set up a predictive profiler of the powder apparent density, presented in *Figure 4.* The curve slopes explain the tendency of the apparent density variations.

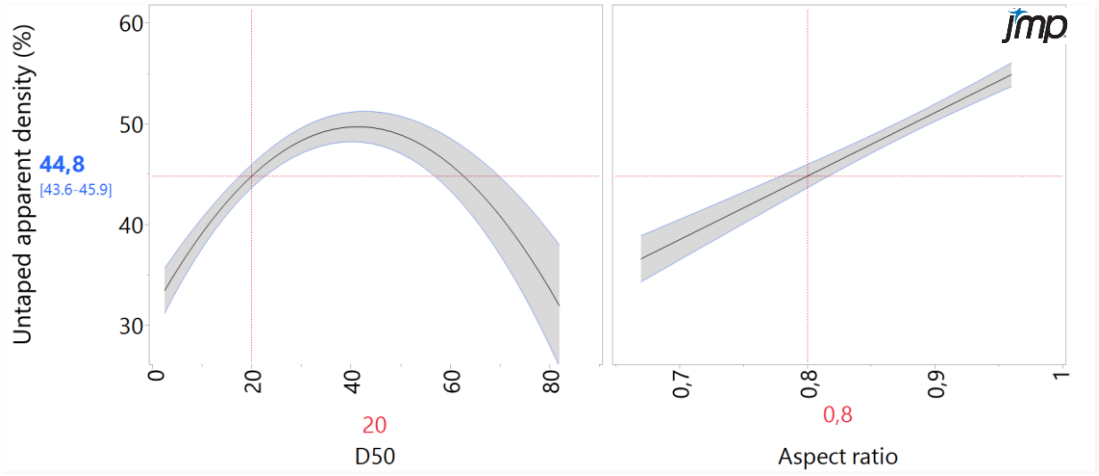

Figure 4: Prediction profiler of powder apparent density (in blue) according to predefined powder characteristics: D50 and Aspect ratio (in red). The grey area displays the 95% confidence interval of the response. The density expressed in %, is a relative apparent density of the theoretical density.

2) Assessment of powder spreading

This section aims to study the correlation between powder characterizations and effective spreadability in PBB-AM machines.

The spreadability of 16 powders from the database has been assessed on a spreading test bench (set up shown in *Figure 5)*. Completely automated, the bench is composed of two pistons enabling powder feeding and powder discharging, with plates of 125x125 mm^2. The spreading tool is mounted on a linear axis. To be representative of most AM equipment's, a rubber blade (with rectangular profile) or a motorized roller (max. rotating speed of 500 rpm) can be adapted on the linear axis.

In order to characterize the powder bed surface, the spreading axis is equipped by a laser profilometer (3200 points/ 16mm line), scanning the surface to reconstitute in 3D the powder bed surface with a x/y resolution of 5 µm and z resolution of 0.5 µm. The cloud of points is then analyzed to extract the average roughness of powder layer. The average roughness (Ra) is calculated for a scanned powder bed surface of 100 x 16 mm^2 (with a cut-off of 2.5 mm, cf. ISO 4287).

In addition, a mass sensor is integrated under the discharging plate (building platform) to calculate the powder layer density *in situ*, with a weighting accuracy of ±10 mg. The layer density is given by averaging 30 weight recordings.

The spreading bench is integrated in a glove box under dry air, to maintain a moisture content under 1000 ppm during experiments (<5 HR%).

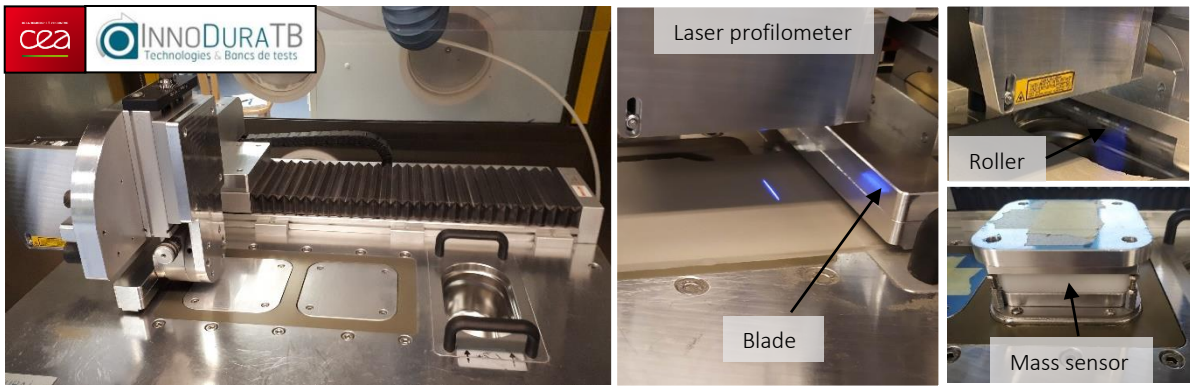

Figure 5: Powder bed test bench developed by CEA/Innodura TB. Details of the laser profilometer, mass sensor and recoaters.

The

Figure 6 presents the correlation matrix between spreadability criteria evaluated in the bench (powder layer roughness and density) and powder characterisations previously presented. These data were obtained for a blade spreading, at 100 mm/s.

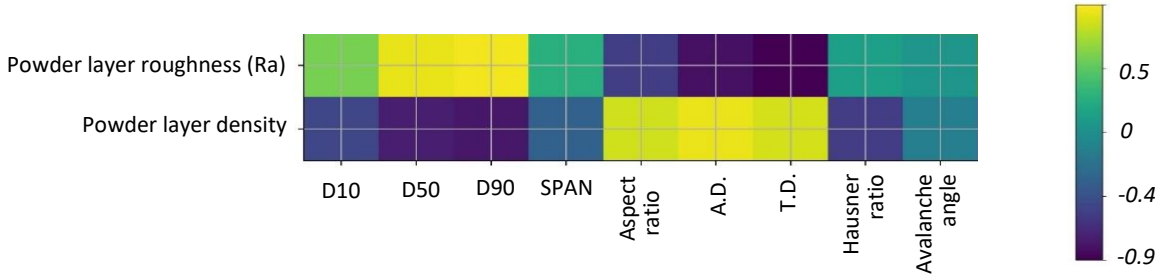

SOSstat	D10	D50	D90	SPAN	Aspect ratio	Untaped density	Taped density	Hausner ratio	Avalanche angle
Powder layer roughness (Ra)	0.61	**0.94**	**0.97**	*	-0.55	**-0.82**	**-0.90**	*	*
Powder layer density	-0.49	**-0.74**	**-0.78**	-0.31	**0.86**	**0.94**	**0.88**	-0.55	-0.08

Figure 6: Linear correlation matrix between spreadability characteristics (powder bed roughness and density) and powder characteristics i.e. D10, D50, D90, SPAN, Aspect ratio, Apparent density (A.D.), Tapped density (T.D.), Hausner ratio (tapped/untapped density) and avalanche angle measurements.
*Bottom: Table of corresponding Pearson coefficient for each linear correlation. Correlations denoted by * are not significantly different from 0.*

Powder layer roughness and powder layer density follow opposite directions according to the different variables (opposite signs of the Pearson coefficients). Consequently, an increase of the layer roughness is inevitably accompanied by a degradation of layer density.

In details, the layer roughness increases while the particle size raises, as well as the powder density (untapped and tapped) decreases. Conversely, the powder layer density is enhanced as the PSD decreases (mainly D50 and D90). Above the PSD, the particle aspect ratio is the main factor influencing the density.

In addition, the powder layer density is strongly related to the powder apparent density characterizations (untapped or tapped). Hence, these ex-situ characterizations are relevant to assess in a first approach the powder spreadability. Finally, the results point out that powder flowability does not affect significantly the layer roughness nor the layer density. Then powder flowability maybe only required for powder feeding phases in AM-processes, in particular the devices using a hopper instead of a feeding piston.

The number of powders assessed up to now on the bench is limited and does not allow to establish an accurate predictive regression of the powder layer density (as performed for the powder apparent density in Section 1).

3) Effect of spreading tool

In this section, a preliminary study is presented to underline the effect of the recoater type on the powder layer properties. As previously mentioned, the results in Section 2 were obtained using a blade-recoater. The average granulometry of the 16 powders assessed in the previous section were higher or equal to 15 microns. Indeed, the experiments show that finer powders are not spreadable with a blade, as these results in a raise of powder layer roughness (*Figure 7)*.

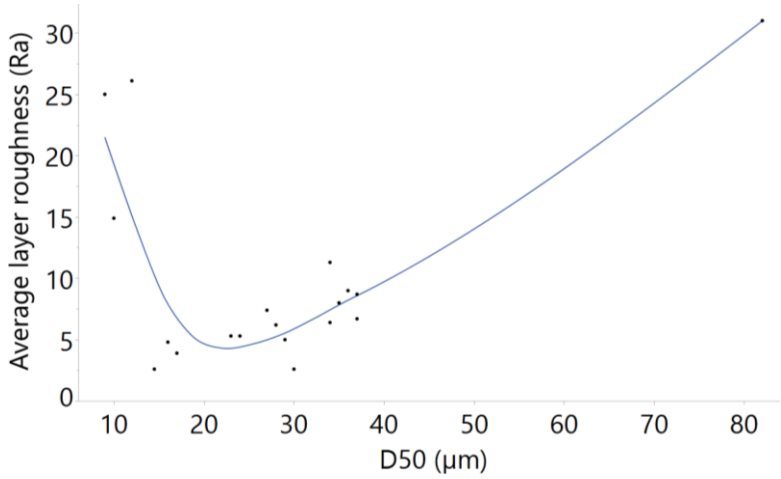

Figure 7: Powder layer roughness according to average PSD (D50) of powders using a blade*.*

Thus, a comparative study using either a blade or a roller recoater is presented, using a fine powder with an average particle size of 9 µm. The *Table 1* shows the main characteristics of the selected powder for this comparison.

	D10	D50	D90	SPAN	Aspect ratio	Untaped density	Taped density	Hausner ratio	Avalanche angle
Powder characteristics	3	9	24	2.3	0.78	32%	63%	1.97	56.9°

Table 1: Characterizations of the "9 µm powder" selected for the blade*/roller comparative.*

The *Figure 8* shows the surface topology of a powder layer spread at 100 mm/s as scanned by the laser profilometry. For this experiment, the rotation speed of the motorized roller is set up at 300 rpm, in counter-clockwise.

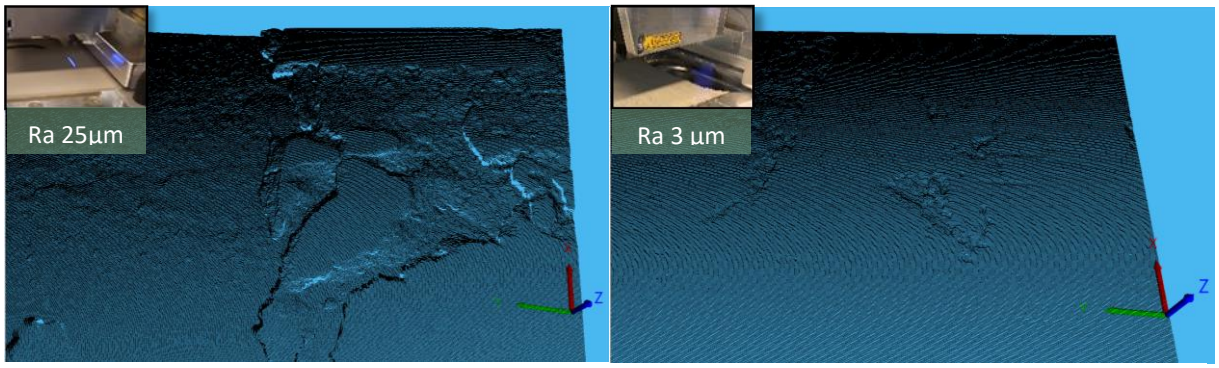

Figure 8: Scans of the powder layers surface for a 9 microns powder using a blade *(left) or a motorized roller at 300 rpm (right), for an equal spreading speed of 100 mm/s and a layer thickness of 60µm.*

Spreading powder with a blade leads to a very uneven surface topology, with many empty patches. The powder is too much cohesive to be compatible with a powder bed-based process using a blade. However, the roughness of the powder layer spread by a roller is much smaller in comparison.
The normal force applied to the roller has a compacting effect on the powder bed, while the blade spreader sustains mainly tangential forces. This compaction effect of the roller helps the particle to rearrange and can improve the powder layer density [13][14][15].

If the spreadability is drastically improved thanks to a roller spreading, it can be noticed that some empty patches are remaining at the layer surface. In addition, the resulting powder layer density is low (37.0 ± 1.5%). The spreadability is here impacted by the limited sphericity of this water-atomized powder (aspect ratio of 0.78, instead of 0.88-0.96 for a gas-atomized powder) and the low powder untapped density (*Table 1*). These two factors are highly correlated to the powder layer density spread by a blade *(*

*Figure **6**)* and the use of roller is not disrupting this statement.

Conclusions and outlook

Cumulative characterization data collected from 59 stainless steel powders have been analyzed in order to better understand and predict powder spreadability in L-PBF and Binder Jetting processes.
To this end, ex-situ characterization have been performed thanks to an assessment of the powder spreadability in an instrumented bench specifically designed for this purpose.
The following conclusions can be drawn:

(1) Powder layer density is mainly driven by powder apparent density and not influenced by powder flowability. The powder apparent density itself is primarily correlated to particle sphericity. Also, a minimal particle aspect ratio of 0.85 is required to achieve layer density higher than 50%.
(2) A predictive model of the powder apparent density according to particle size and shape is set up in this study. This analytical model is relevant to screen powder spreadability as a first approach, and without experiments.
(3) The powder layer roughness is decreasing with the reduction of the particle size (D50, D90). Particle sphericity must be enhanced simultaneously to the particle size reduction to maintain the powder apparent density higher than 50% (to overcome the cohesive contribution of a PSD reduction). Then powders having fine particle size between 15-30 µm in D50 and aspect ratio from 0.90 to 0.95 exhibit at the same time smooth powder layer (Ra ≤5µm) and high powder apparent density (≥ 50%).
(4) Under average particle size of 15 µm, roller recoater is required to ensure the spreading of layers free-off empty patches.

The upcoming developments will consist in the development of a statistic predictive model of the powder layer density based not only on powder characteristics (shape and size), but also on process parameters that will be implemented in the model: powder layer thickness, recoater speed, type of recoater (blade or roller).

References

[1] L. Hitzler *et al.*, A Review of Metal Fabricated with Laser- and Powder-Bed Based Additive Manufacturing Techniques: Process, Nomenclature, Materials, Achievable Properties, and its Utilization in the Medical Sector, Advanced Engineering Materials, 20 (2018). https://doi.org/10.1002/adem.201700658.
[2] M. Ziaee *et al.*, Binder jetting: A review of process, materials, and methods, Additive Manufacturing 28 (2019) 781–801. https://doi.org/10.1016/j.addma.2019.05.031
[3] Particle packing characteristics by Randall M. German, 1989, Metal Powder Industries Federation edition
[4] X. Jia *et al.*, A packing algorithm for particles of arbitrary shapes, Powder Technology 120 (2001) 174-186.https://doi.org/10.1016/S0032-5910(01)00268-6
[5] M. Soulier *et al.*, Analytical and Numerical Modelling of Stainless Steel Powders Spreading in Powder-Bed Processes for Additive Manufacturing, Conference paper Euro PM 2021.
[6] C. Meier *et al.*, Critical influences of particle size and adhesion on the powder layer uniformity in metal additive manufacturing, Journal of Materials Processing Technology 266 (2019) 484-501.https://doi.org/10.1016/j.jmatprotec.2018.10.037
[7] K. Marchais *et al.*, A 3D DEM simulation to study the influence of material and process parameters on spreading of metallic powder in additive manufacturing, Computational Particle Mechanics 8 (2021) 943-953. https://doi.org/10.1007/s40571-020-00380-z
[8] A. Anand *et al.*, Predicting discharge dynamics from a rectangular hopper using discrete element method (DEM), Chemical Engineering Science 63 (2008) 5821—5830. 10.1016/J.CES.2008.08.015
[9] N. Vlachos *et al.*, Investigation of flow properties of metal powders from narrow particle size distribution to polydisperse mixtures through an improved Hall-flowmeter, Powder Technology 205 (2001) 71-80. https://doi.org/10.1016/j.powtec.2010.08.067
[10] E. Vasquez *et al.*, Effect of powder characteristics on production of oxide dispersion strengthened Fe- 14Cr steel by laser powder bed fusion, Powder Technology 360 (2020) 998–1005. https://doi.org/10.1016/j.powtec.2019.11.022

[11] M. Soulier *et al.*, Study of 316L stainless steel powders specifications on parts printed by laser-powered -powder bed fusion (PBF), Conference paper Euro PM 2018.
[12] M. Soulier *et al.*, Analytical And Numerical Modeling Of Stainless Steel Powders Spreading In Powder-Bed Processes For Additive Manufacturing, Conference paper Euro PM 2021.
[13] S. Haeri *et al.,* Optimisation of blade type spreaders for powder bed preparationin additive manufacturing using dem simulations. Powder Technology (2017) 321,94–104. *https://doi.org/10.1016/j.powtec.2017.08.011*
[14] L. Wang *et al.*, Adhesion effects on spreading of metal powders in selective laser melting. Powder Technology (2020) 363, 602–610. https://doi.org/10.1016/j.powtec.2019.12.048
[15] J. Zhang *et al.*, Comparison of roller-spreading and blade-spreading processes inpowder-bed additive manufacturing by DEM simulations, Particuology 66 (2022) 48-58 https://doi.org/10.1016/j.partic.2021.07.005